Supplementary Figure S1

A)

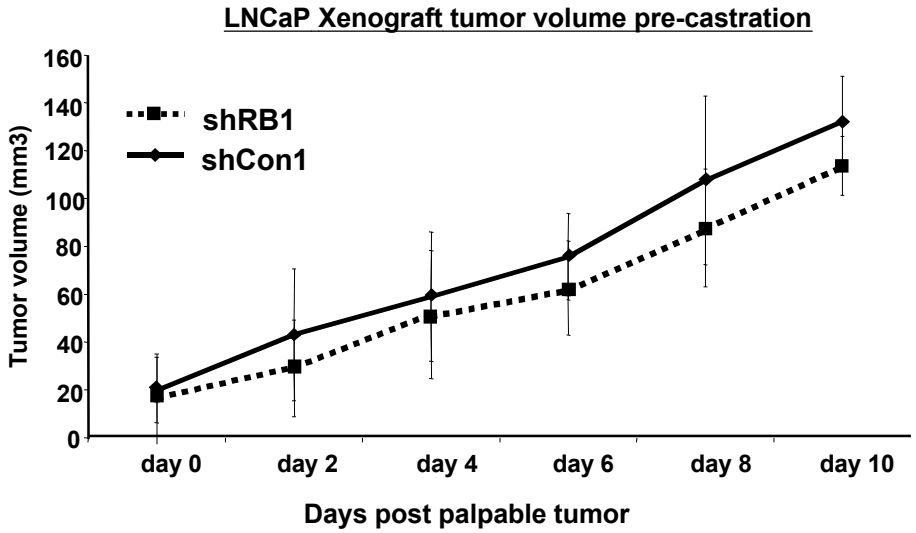

B)

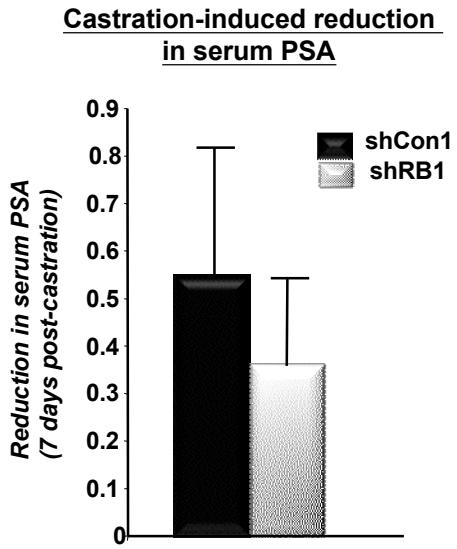

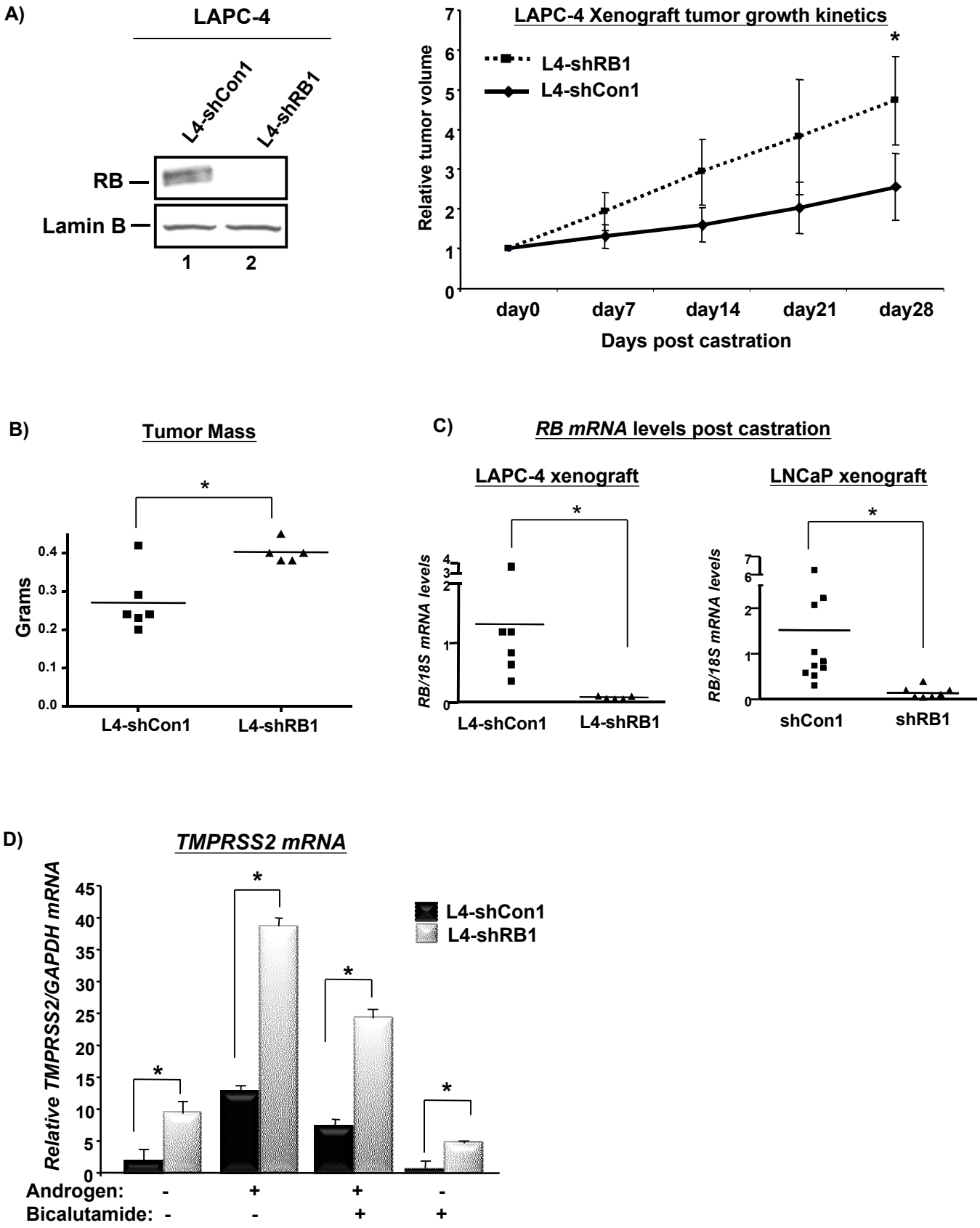
A)
LAPC-4
L4-shCon1
L4-shRB1
RB
Lamin B
1
2
LAPC-4 Xenograft tumor growth kinetics
L4-shRB1
L4-shCon1
Relative tumor volume
day0
day7
day14
day21
day28
Days post castration
B)
Tumor Mass
Grams
L4-shCon1
L4-shRB1
C)
RB mRNA levels post castration
LAPC-4 xenograft
LNCaP xenograft
RB/18S mRNA levels
L4-shCon1
L4-shRB1
shCon1
shRB1
D)
TMPRSS2 mRNA
Relative TMPRSS2/GAPDH mRNA
L4-shCon1
L4-shRB1
Androgen:
Bicalutamide:

Supplementary Figure S3

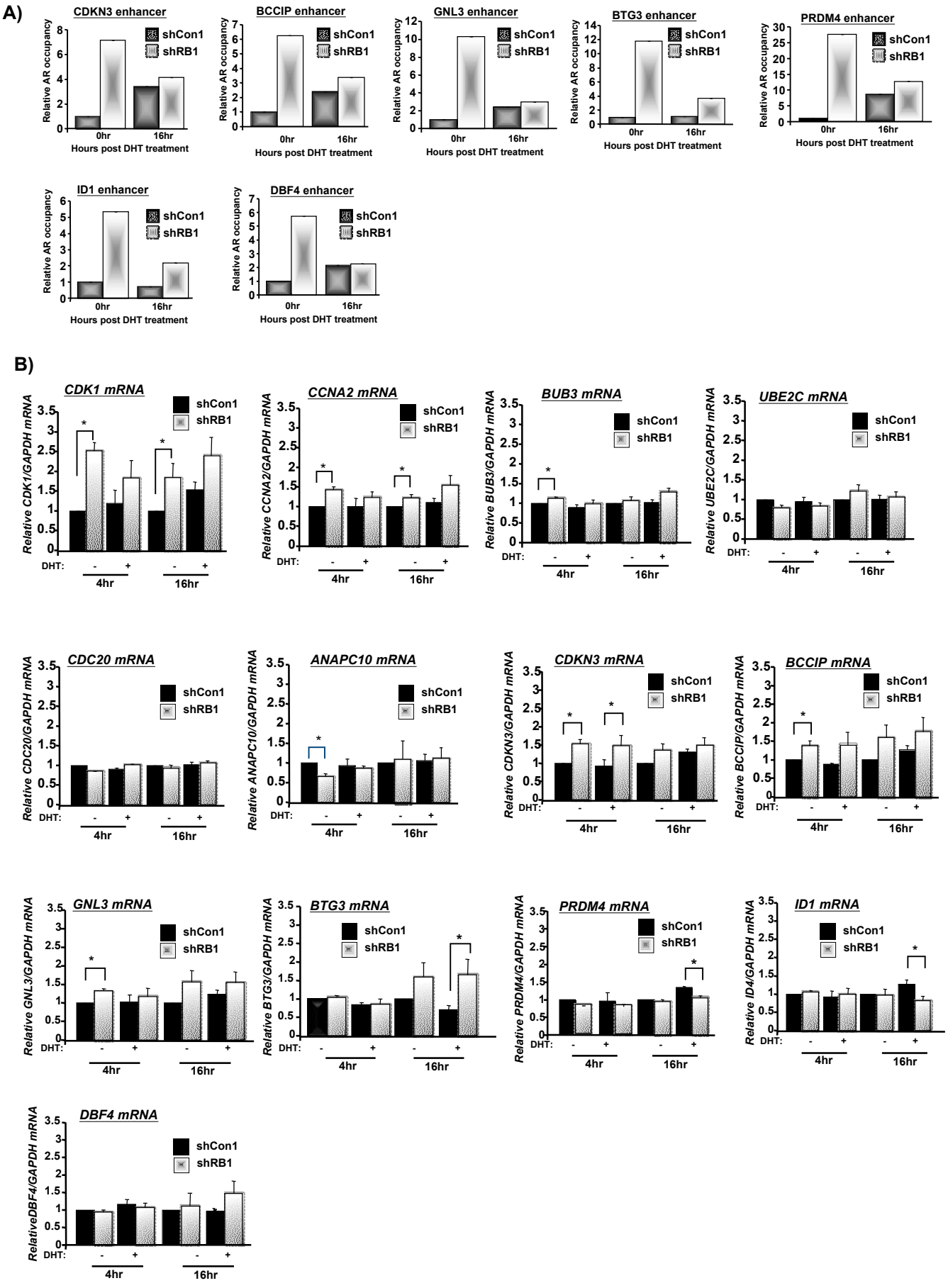

Supplementary Figure S4

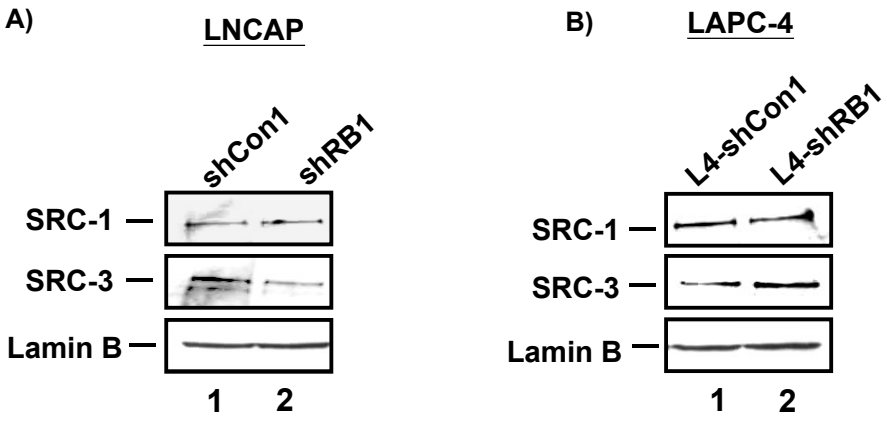

Supplementary Figure S5

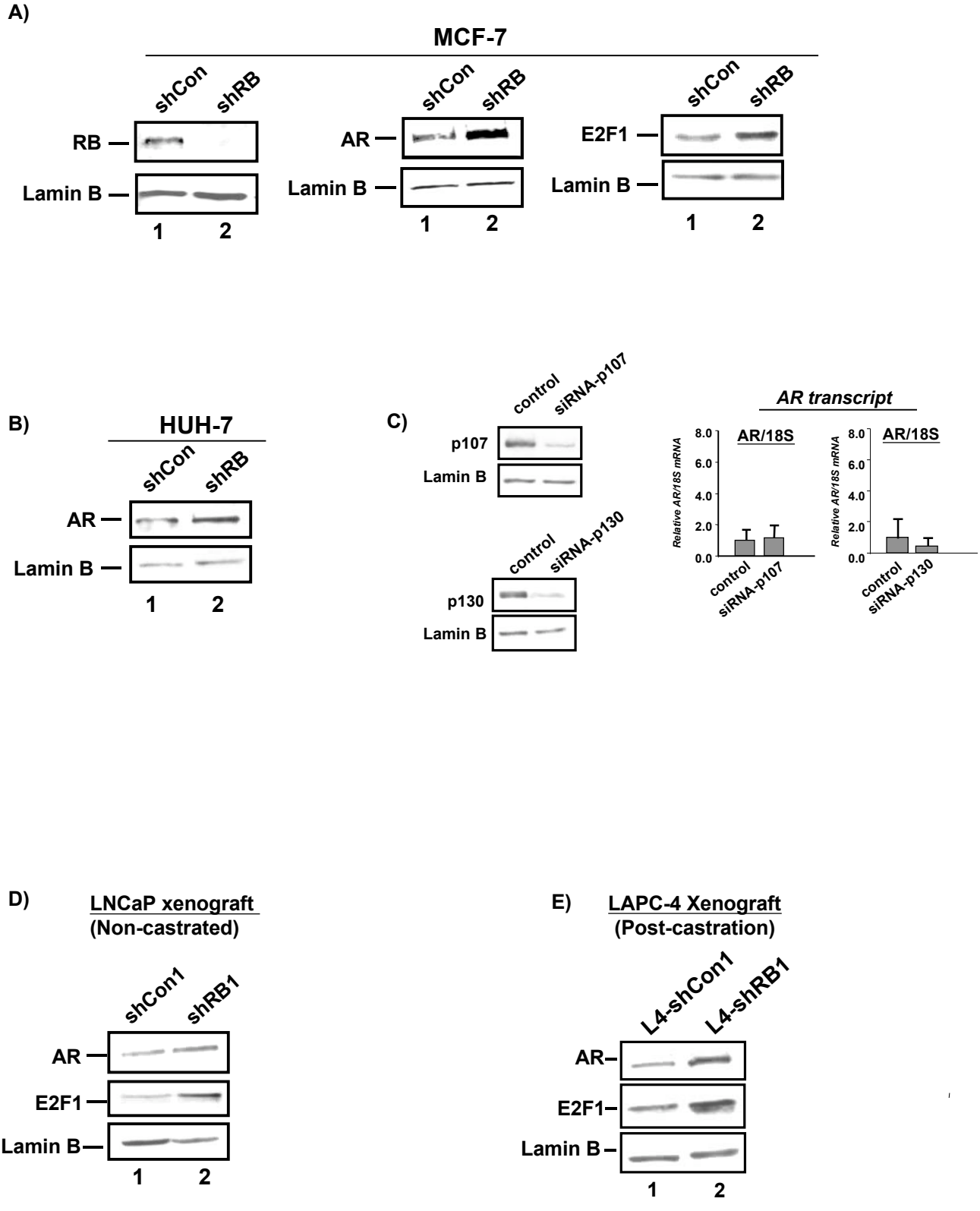

Supplementary Figure S6

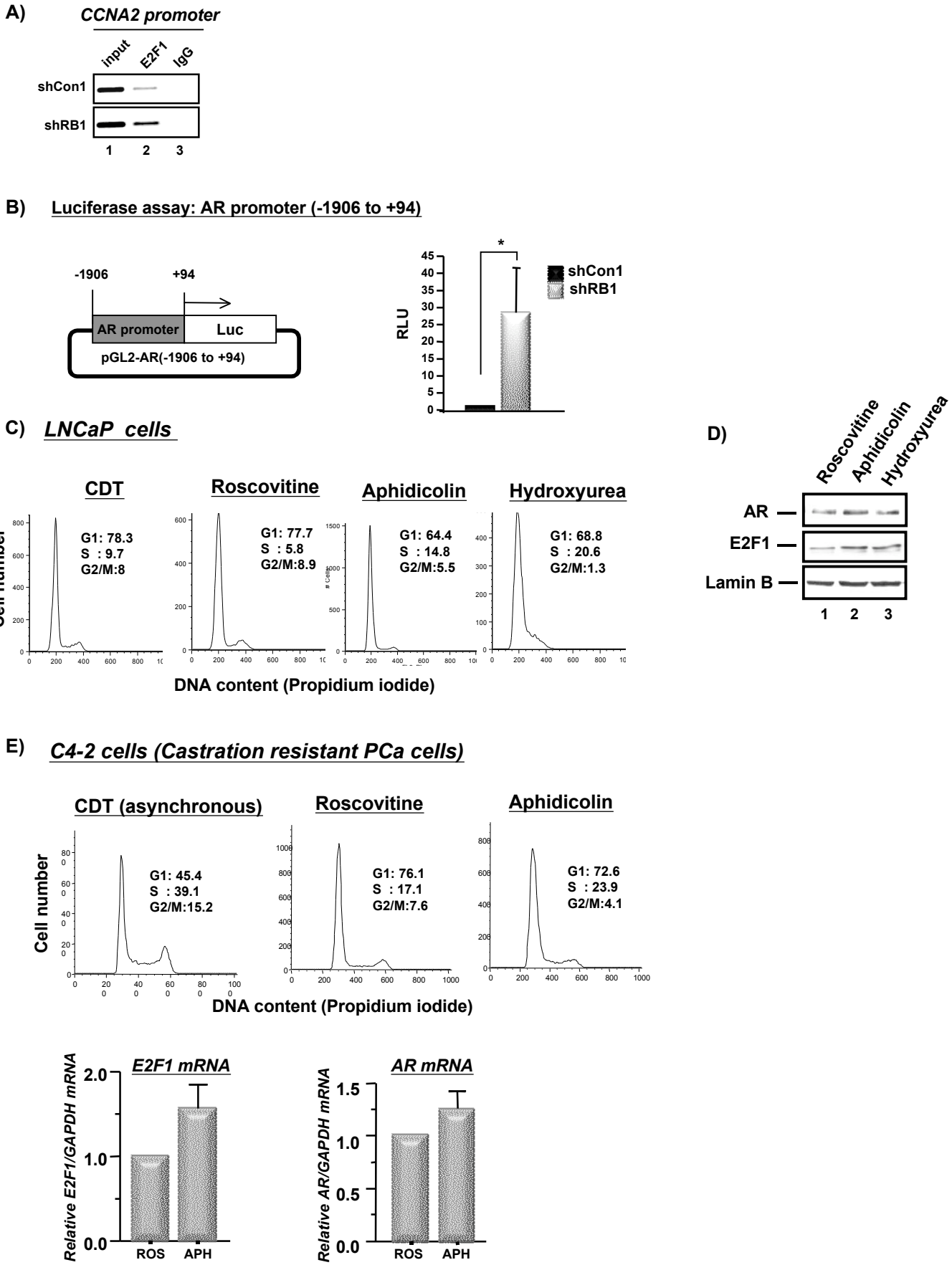

Supplementary Figure S7

A)

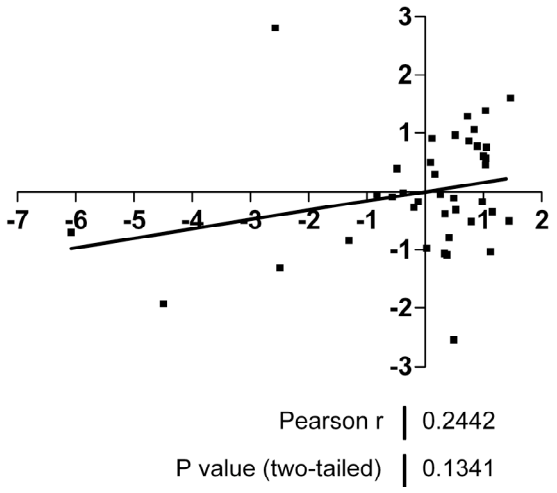

B)

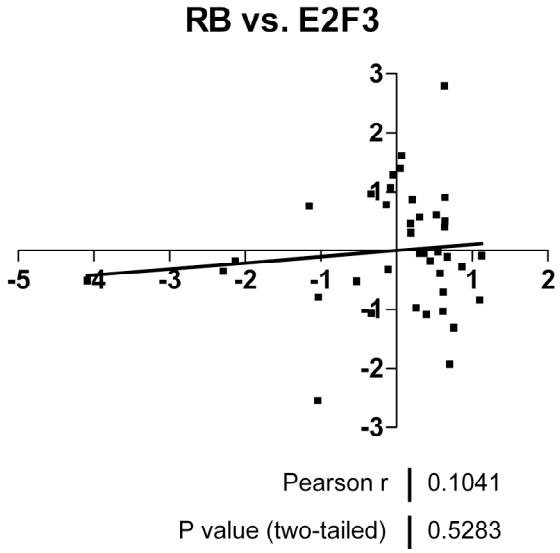

Supplementary Figure S8

A)

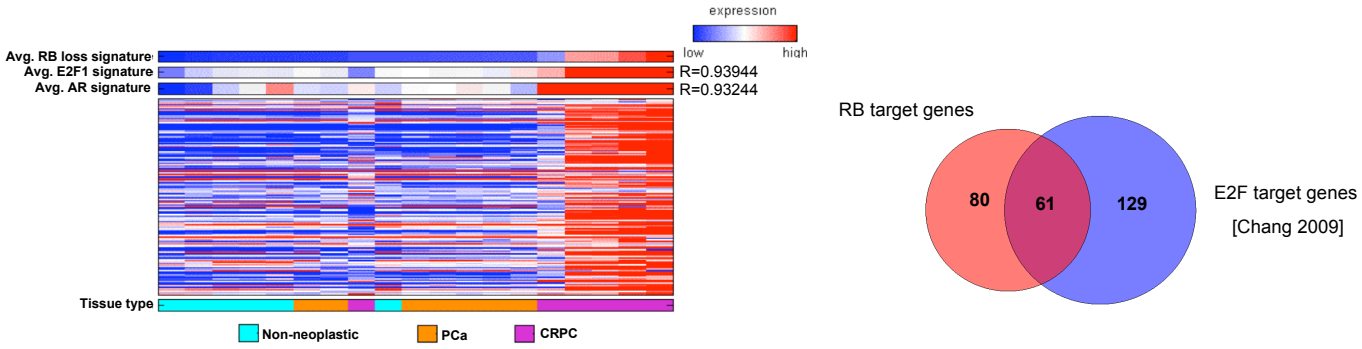

B)

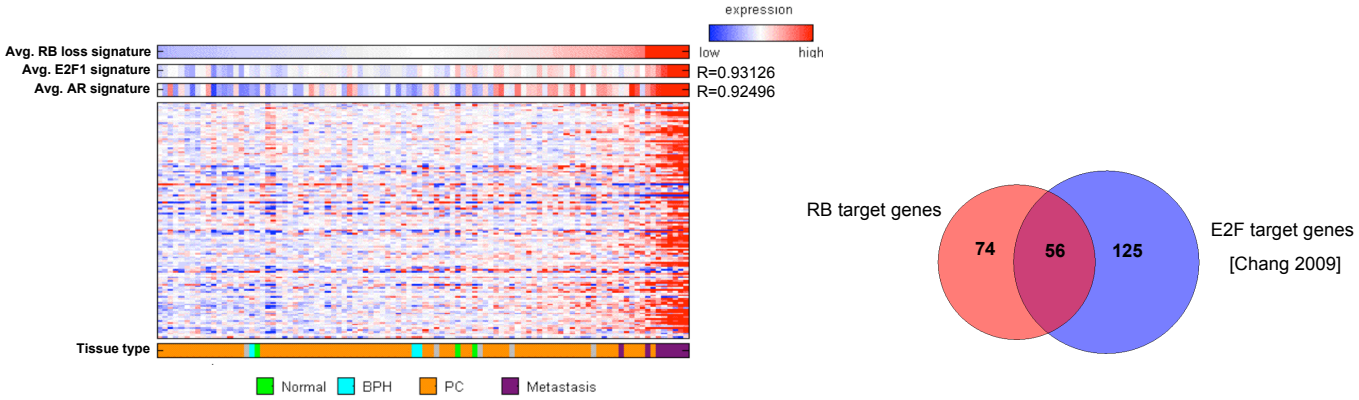

Supplementary table S2

GENE	SEQUENCE (5' to 3')
PSA (forward)	GACCAAGTTCATGCTGTGTG
PSA (reverse)	ACTAGGGAGCCATGGAGGAC
TMPRSS2 (forward)	GTGATGGTATTCACGGACTGG
TMPRSS2 (reverse)	CAGCCCCATTGTTTTCTTGTA
GAPDH (forward)	GAGTCAACGGATTTGGTCGT
GAPDH (reverse)	GACAAGCTTCCCGTTCTCAG
E2F1 (forward)	TATGGTGATCAAAGCCCCTC
E2F1 (reverse)	AGATGATGGTGGTGGTGACA
AR (forward)	AAGACCTGCCTGATCTGTGGAG
AR (reverse)	CCCAGAGTCATCCCTGCTTCAT
RB (forward)	GGAAGCAACCCTCCTAAACC
RB (reverse)	TTTCTGCTTTTGCATTCGTG
CCNA2 (forward)	AGACGGGTTGCACCCCTTA
CCNA2 (reverse)	TTTTTGAGATTCAGCTGGCTTCT
18S (forward)	GCAATTATTCCCCATGAACG
18S (reverse)	GGCCTCACTAAACCATCCAA

Supplementary table S3

LOCUS	**SEQUENCE (5' to 3')**
Region 1 (forward)	TGGTGATGTGGAAGCAACATA
Region 1 (reverse)	GGTCTCAGAGCCAGGAGAACT
Region 2 (forward)	GCCATTAAAATCTCAGGAAATAAT
Region 2 (reverse)	AAACTAGTCTTCCAGTCCATTGC
Region 3 (forward)	TAAAGCTACAACAAAGCTACAACC
Region 3 (reverse)	CCTGGGCCTCCCTATGTTTT
Region 4 (forward)	GTCCATCAAGAGGCGAAAAG
Region 4 (reverse)	TCCAGACTCTCAAAGGCAAAA
Region 5 (forward)	CTGCGCGCTCTTATCAGTC
Region 5 (reverse)	CCCCTGCTTCCTGAATAGC
Region 6 (forward)	AGGTGGGAAGGCAAGGAG
Region 6 (reverse)	TAGCTCGGCCCTTTTTCC
E2F1 consensus region (forward)	CCCATTCATTACCACGAGGA
E2F1 consensus region (reverse)	CCCCACTAAGTCTCATGTTGAA
ALB (Albumin) promoter (forward)	CAGGGATGGAAAGAATCCTATGCC
ALB (Albumin) promoter (reverse)	CCATGTTCCCATTCCTGCTGT
CCNA2 promoter (forward)	CCCCAGCCAGTTTGTTTCT
CCNA2 promoter (reverse)	AGTTCAAGTATCCCGCGACT

Supplementary figure legends

Figure S1: RB depletion confers no tumor growth advantage in intact male mice but alters biochemical response to castration in vivo.

A. Tumor volume in unchallenged shRB1 and shCon1 xenografts from Figure 3A, measured upon palpable tumor detection and at indicated days prior to castration. **B.** Reduction in serum PSA levels from day of castration (day 0) to nadir point (day 7) in each cohort ($p>0.05$, Student's t-test).

Figure S2: RB disruption confers castration resistance and increases AR activity in multiple prostate cancer model systems.

A. Left panel: Immunoblot analysis to assess levels of RB in RB proficient (L4-shCon1) and deficient (L4-shRB1) LAPC-4 cells. Right panel: Relative tumor volume of L4-shCon1 and L4-shRB1 xenografts post castration. Host animals were castrated at 100-150mm^3 (day 0). Data plotted is mean tumor size $\pm$ SD for each cohort (n=6 for shCon1 and n=5 for shRB1). **B.** Tumor weight on sacrifice (day 28), from tumors followed in panel A. **C.** RB mRNA levels in L4-shCon1 (n=6) and L4-shRB1 (n=5) xenograft tumors and shCon1 (n=10) and shRB1 (n=7) xenograft tumors post castration. **D.** TMPRSS2 mRNA levels in L4-shCon1 and L4-shRB1 cells measured using methods identical to those described for Figure 3F. (*$p<0.05$, Student's t-test).

Figure S3: RB depletion alters AR occupancy at cell cycle genes.

A. ChIP analyses of basal and 16 hrs post-DHT stimulated AR occupancy at enhancer regions of CRPC enriched, AR target genes not directly associated with mitosis (*CDKN3*, *BCCIP*, *GNL3*, *BTG3*, *PRDM4*, *ID1* and *DBF4*) in shRB1 and shCon1 cells. Methodology was identical to that described for Figure 4B, and primer sequences were identical to those previously described (1). **B.** Basal and DHT stimulated (4hrs and 16hrs) expression levels of various M-phase and non M-phase genes in shCon1 and shRB1 cells measured using qPCR. Primer sequences were identical to those described previously (1). Results are plotted for each treatment condition relative to that in shCon1 in CDT set to "1". Values represent triplicate analyses of three independent biological replicates (mean$\pm$ S.D, *$p<0.05$, Student's t-test).

Figure S4: RB depletion does not deregulate SRC coregulator expression levels.

SRC-1 and SRC-3 protein levels were determined in LNCaP (panel **A**) and LAPC-4 (panel **B**) cells after RB knockdown, as indicated. Lamin B was used as loading control.

Figure S5: RB depletion deregulates AR and E2F1 expression.

A. Immunoblot analysis to assess levels of RB (left panel), AR (middle panel) and E2F1 (right panel) in MCF-7 breast cancer cells transfected with shRB or control shRNA. **B**. AR levels in RB proficient and deficient HUH-7 liver cancer cells. **C.** Left: Immunoblot analysis to verify knockdown of p107 and p130 in LNCaP cells. Right: Q-pcr analysis of *AR* transcript levels post p107 and p130 knockdown. **D and E**. AR and E2F1 levels from representative non-castrated shCon1 and shRB1, and castrated L4-shCon1 and L4-shRB1 xenograft tumor cohorts, respectively. Lamin B was used as the loading control.

Figure S6: RB depletion alters E2F1 binding at *CCNA2* promoter, increases AR promoter reporter activity, and AR and E2F1 are regulated as a function of G1/S phase.

A. ChIP analysis of E2F1 binding to the *CCNA2* promoter region in shCon1 and shRB1 cells. These experiments were performed in parallel with those described in Figure 6A. **B.** Left panel: Schematic of AR promoter reporter construct. Right panel: AR reporter luciferase activity measured in shCon1 and shRB1 cells cultured in androgen proficient media. (*p<0,05, Student's t-test). **C**. Flow cytometric analyses as described in Figure 6C. **D.** Immunoblot analysis to measure AR and E2F1 protein levels in cells treated in panel C. Lamin B served as the loading control. **E**. Representative flow cytometric traces and qPCR analyses to monitor *E2F1* (left) and *AR* (right) mRNA from C4-2 cells cultured in CDT media and arrested in G1 (ROS) and early S-phase (APH). Transcript levels in ROS treated condition was set to "1". Data represent triplicate analyses of at least 2 independent biological replicates assessed in triplicate (mean $\pm$ S.D).

Figure S7: AR and RB expression directly correlate with E2F3 levels in castrate resistant prostate cancer specimens.

Log_2 scaled expression ratio of *AR versus E2F3* (top graph) and *RB versus E2F3 (bottom graph)* from 39 human castrate resistant metastases. ($p>0.05$, Student's t-test)

Figure S8: RB-loss signature genes show commonality with E2F targets.

A. The heatmap (left) is reproduced from Figure 1B and depicts prostate tissue samples from Varambally data set (2) ordered from left to right based on relative representation of the RB loss signature (top bar). Horizontal expression bars also show average E2F signature (3) and average AR signature (1). The Venn diagram (right) depicts the relationship between the sets of RB loss signature genes and E2F targets from (3) for genes represented in this dataset on the HGU133 plus 2 platform. **B.** The heatmap (left) is reproduced from Figure 1C and depicts prostate tissue samples from (4) ordered from left to right based on relative representation of the RB loss signature (top bar). Horizontal expression bars also show average E2F signature and average AR signature. Bars are labeled with the Pearson correlation coefficient representing their similarity compared to the RB loss signature. Sample type is provided on the bottom bar. The Venn diagram (right) depicts the relationship between the sets of RB loss signature genes and E2F targets for genes represented in this dataset on the HGU133A platform.

Supplemental Methods:

Cell lines and xenografts: Cells were passaged in media containing 5% fetal bovine serum (FBS), but for androgen deprivation conditions were cultured in charcoal dextran treated FBS (CDT, purchased from and validated by Hyclone), supplemented when indicated with the bicalutamide (Bic). Athymic, nude mice were purchased from the National Cancer Institute-Frederick Cancer Research Facility (Frederick, MD) and housed in cages fitted with a high efficiency filter top in animal facilities approved by the American Association for Accreditation of Laboratory Animal Care. Once tumors reached 100 to 150 mm^3, the mice were surgically castrated. Blood was drawn through weekly retro-orbital eye bleed for

serum PSA analyses. After 28 days post castration, mice were euthanized, at which point tumors were harvested, weighed and stored for subsequent RNA and protein analyses.

Assessment of RB transcript levels in xenograft tumors: Quantification of RB levels in xenograft tumors was determined by qPCR using human RB specific primers. RB levels were normalized to the respective endogenous control (18S) using the formula $\Delta C_t = C_t$ (RB)-C_t (18S). Comparative $\Delta\Delta C_t$ values (difference between ΔC_t for each mouse in RB proficient and deficient cohorts and average ΔC_t for RB proficient cohort) were used to calculate levels ($=2^{-\Delta\Delta Ct}$) of RB transcript.

Knockdowns, transfections, and infections: Vector-delivered shRNA and control targeting sequences used to knockdown RB (5'-CGCATACTCCGGTTAGGACTGTTATGAA-3') in LNCaP cells and (5_-GAAAGGACATGTGAACTTA-3') in LAPC-4 cells have been previously described (5). For siRNA studies, sequences used for E2F1 were: *siE2F1* sense, 5'-UGGACCACCUGAUGAAUAUdTdT-3'; and antisense, 5'-AUAUUCAUCAGGUGGUCCAdTdT-3' (6). The siRNA sequences used for AR were: *siAR* sense, 5'-GACUCAGCUGCCCCAUCCAdTdT-3'; and antisense, 5'- UGGAUGGGGCAGCUGAGUCdTdT-3' (7). Control siRNA (siNS) was validated Allstars Negative Control (Cat No 1027281, Qiagen, Valencia, CA). For p107/p130 knockdown studies, LNCaP cells were plated in androgen proficient media. After 24 hrs, cells were transfected with ON-TARGETplus SMARTpool siRNA against p107 (L-003298-00-0005) or p130 (L-003299-00-0005) and ON-TARGETplus non-targeting pool (D-001810-10-20) from Dharmacon. Cells were harvested 48-72 hrs post transfection and subjected to immunoblot and qPCR analyses to assess the levels of p107, p130 and AR mRNA. For shRNA vector transfection experiments, cells were transfected under serum free conditions with the indicated plasmids. Following transfection, cells were supplemented with media containing FBS for 48hr, after which the cells were harvested and RNA isolated. For viral infection studies, cells were transduced in media containing 5% FBS with adenovirus encoding GFP, E2F1, E2F2 and E2F3. After 24 hr, cells were harvested, and RNA and protein isolated. For AR and E2F1 knockdown studies, cells were plated in androgen proficient media (IMEM with 5% FBS) in poly-L-lysine coated plates. Cells were then transfected with 200nM of siRNA using

Lipofectamine 2000 (Invitrogen, Carlsbad, CA) for 3 days after which the cells were trypsinized, washed twice with PBS, and subjected to immunoblot analyses to validate the knockdown of AR or E2F1. Parallel dishes were seeded for growth assays in CDT (phenol red-free IMEM with 5% charcoal-stripped FBS). Cell growth in control and siRNA transfected shRB1 was then measured at indicated days using trypan blue exclusion method.

AR promoter cloning and reporter assay: The AR promoter (-1906 to +94) was amplified from genomic DNA of LNCaP cells with FastStart High Fidelity PCR System (Roche, Indianapolis, IN). The PCR primers used were N1906F (GTTGGTGATGTGGAAGCAAC) and P94R (TAGCTCGGCCCTTTTTCC). The 2kb PCR product was cloned into pCR2.1-TOPO (Invitrogen, Carlsbad, CA) to create pCR2.1-AR and the promoter sequence integrity was validated by sequencing with M13 reverse and forward primers. The HindIII-XhoI fragment of AR (+94 to -1906) was cloned into the XhoI-HindII site of pGL2-Basic vector to create pGL2-AR (-1906 to +94) luciferase reporter. For the reporter assay, shCon1 and shRB1 cells were plated in androgen proficient media in poly-L-lysine coated 24-well plate and allowed to grow overnight. Each well was co-transfected with 400 ng luciferase reporter vector (pGL2-Basic or pGL2-AR (-1906 to +94) and 20ng of CMV-β-gal. The cells were incubated with plasmid-Lipofectin (Invitrogen, Carlsbad, CA) complex in serum and antibiotic-free media for 8h at 37C before serum was added to a final concentration of 5% and incubated for 24h at 37C. The cell monolayer was washed twice with PBS and incubated in CDT media containing either ethanol or 10nM DHT. After 24h, the cell monolayer was washed twice with PBS and lysed with reporter lysis buffer (Promega, Madison, WI). Luciferase assay (Promega, Madison, WI) and chemilumiscent β-galactosidase assay (Tropix Galacto-Star, Applied Biosystems, Bedford, MA) were performed as per manufacturer's recommendations and measured with the Zylux Femtometer FB12 luminometer (Zylux, Huntsville, AL). Each sample's luciferase value was normalized to its respective β-galactosidase control. Relative luciferase units (RLU) were then calculated for shCon1 and shRB1 cells in DHT treated condition relative to no ligand treated condition. RLU for shCon1 was then set to "1" and shRB1 plotted relative to this parameter. (*$p<0.05$, Student's t-test).

Flow Cytometric and transcript analyses: Castrate resistant C4-2 cells were plated on poly-L-lysine coated plates in CDT and treated with roscovitine (2.5ug/ml) and aphidicolin (3ug/ml) for 24 hrs to arrest cells in G1- and early S-phase, respectively. Cells were harvested for RNA isolation using Trizol or fixed in ice cold 100% ethanol for cell cycle analyses. Cell cycle analyses was performed by gently re-suspending the ethanol-fixed pellets in 500ul of PBS containing 30uM propidium iodide and 40ug/ml RNase A, following a 10-15min incubation in the dark, cells were processed using a Beckman CoulterXL. Profile analysis was performed using FlowJo (v8.8.6) and profiles (15,000 events) were subjected to the Cell Cycle module and fitted using the Watson Pragmatic model. Representative profiles had an RMS value <3.0. Expression analysis was performed using cDNA generated from either the Superscript III or VILO system (Invitrogen). Quantitative PCR for AR and E2F1 with GAPDH as loading control (Primers described in Supplemental Table S2) was performed using a StepOnePlus machine with Power SYBR (ABI). AR or E2F1 levels in Roscovitine treated condition were set to "1".

Analyses of RB loss signature and RB1: The RB loss signature consists of 159 genes that were previously identified indicative of RB loss in other model systems (largely fibroblasts and hepatocyctes) (8, 9). Thus, this signature represents the "common denominator" of genes deregulated upon RB loss or depletion across multiple tissue types. Pertinent to this study, AR and related target genes are not part of the signature, as would be expected based on the tissues used to derive the gene set. The RB signature was then analyzed with two previously described microarray datasets. The first, which consists of Affymetrix HG-U133 plus2 microarrays, representing benign prostate tumor, clinically localized prostate cancer, and (castrate-resistant) metastatic prostate cancer tissue (2), was downloaded from the Gene Expression Omnibus (GEO) (10) under accession number GSE3325. The second dataset consists of Affymetrix HG-U133A microarrays, including normal prostate, benign prostate tumor, clinically localized prostate cancer, and metastatic prostate cancer, was obtained from Dr. W. Gerald (4, 11). Raw CEL files were processed for each dataset separately, using the RMA Express version 1.0 implementation of the Robust Multichip Average (RMA) procedure (12). Custom CDFs, dated July 30, 2009 (version 12), containing alternative Entrez Gene probeset definitions for the HG-U133A and HG-

U133 plus 2 platforms (13) were used to provide consistency with current transcript definitions and improve annotation quality. The resulting RMA expression values were saved in log2 scale and imported into MATLAB software (The MathWorks, Inc., Natick, MA) for further analysis. The RB signature genes were mapped to each array platform, with 130 out of 159 RB signature genes represented on the HG-U133A platform and 141 out of 159 represented on the HG-U133 plus2 platform. Gene transcript profiles representing the RB target signature in each dataset were median-centered and averaged to create a single profile representative of the overall RB target signature magnitude. Expression levels for the *RB1* transcript and the RB target signature average profile were compared between benign, clinically localized, and metastatic prostate cancer tissue from the Varambally dataset using box and whisker plots. The same comparison was performed between clinically localized and metastatic prostate cancer tissue from the Gerald dataset. P-values for differential expression between metastatic and clinically localized tumor were calculated using a two-sided t-test. Heatmaps were generated for the RB signature in each dataset ordering samples by the RB loss signature average value. For the recurrence free survival data, 79 primary tumor samples in the Gerald dataset were used to evaluate the prognostic significance of the RB-loss signature. Samples were categorized into lower, intermediate, and upper quartile ranges of RB-loss signature magnitude and the Kaplan-Meier survival curves were generated for each of these expression categories. Differences in recurrence-free survival among the three expression categories were evaluated for significance using the log-rank test.

Analyses of E2F1 and AR signatures: A 224-gene signature representative of E2F targets was obtained from the Supplemental Table S4 in (3). Official gene symbol was used to match 190 of these genes to the HGU133 plus 2 array and 181 of these genes to the HGU133A array. Similarly, a signature of 38 genes regulated by AR in androgen independent prostate cancer was obtained from supplemental table S2 in (1) and mapped to 34 genes on the HGU133 plus 2 array and 31 genes on the HGU133A array. In the both the Varambally (HGU133 plus 2) and Glinsky (HGU133A) datasets, gene profiles corresponding to the E2F and AR target signatures were median-centered and averaged to create a

single profile. These profiles were compared with the RB loss signature using the Pearson correlation coefficient.

AR, RB, E2F1, and E2F3 expression in castrate-resistant human prostate tumors: Agilent 44K whole human genome expression oligonucleotide microarrays (Agilent Technologies, Inc.) were used to profile 39 human castration-resistant soft tissue metastases of prostate adenocarcinomas from nine patients described (14). The tumor samples were all laser-capture microdissected, and total RNA isolated and amplified as described previously (15). Probe labeling and hybridization was performed following the Agilent suggested protocols and fluorescent array images were collected using the Agilent DNA microarray scanner G2565BA. Agilent Feature Extraction software was used to grid, extract, and normalize data. Expression ratios were $\log_2$ scaled and mean-centered across each gene. GraphPad Prism v4.03 software was used to analyze the correlation of expression between genes. A Pearson correlation coefficient, linear regression, and F test for significantly non-zero slope was performed for each pair of genes.

Supplemental References

1. Wang, Q., Li, W., Zhang, Y., Yuan, X., Xu, K., Yu, J., Chen, Z., Beroukhim, R., Wang, H., Lupien, M., et al. 2009. Androgen receptor regulates a distinct transcription program in androgen-independent prostate cancer. *Cell* 138:245-256.
2. Varambally, S., Yu, J., Laxman, B., Rhodes, D.R., Mehra, R., Tomlins, S.A., Shah, R.B., Chandran, U., Monzon, F.A., Becich, M.J., et al. 2005. Integrative genomic and proteomic analysis of prostate cancer reveals signatures of metastatic progression. *Cancer Cell* 8:393-406.
3. Chang, J.T., Carvalho, C., Mori, S., Bild, A.H., Gatza, M.L., Wang, Q., Lucas, J.E., Potti, A., Febbo, P.G., West, M., et al. 2009. A genomic strategy to elucidate modules of oncogenic pathway signaling networks. *Mol Cell* 34:104-114.
4. Glinsky, G.V., Glinskii, A.B., Stephenson, A.J., Hoffman, R.M., and Gerald, W.L. 2004. Gene expression profiling predicts clinical outcome of prostate cancer. *J Clin Invest* 113:913-923.

5. Bosco, E.E., Wang, Y., Xu, H., Zilfou, J.T., Knudsen, K.E., Aronow, B.J., Lowe, S.W., and Knudsen, E.S. 2007. The retinoblastoma tumor suppressor modifies the therapeutic response of breast cancer. *J Clin Invest* 117:218-228.

6. Stender, J.D., Frasor, J., Komm, B., Chang, K.C., Kraus, W.L., and Katzenellenbogen, B.S. 2007. Estrogen-regulated gene networks in human breast cancer cells: involvement of E2F1 in the regulation of cell proliferation. *Mol Endocrinol* 21:2112-2123.

7. Compagno, D., Merle, C., Morin, A., Gilbert, C., Mathieu, J.R., Bozec, A., Mauduit, C., Benahmed, M., and Cabon, F. 2007. SIRNA-directed in vivo silencing of androgen receptor inhibits the growth of castration-resistant prostate carcinomas. *PLoS One* 2:e1006.

8. Markey, M.P., Angus, S.P., Strobeck, M.W., Williams, S.L., Gunawardena, R.W., Aronow, B.J., and Knudsen, E.S. 2002. Unbiased analysis of RB-mediated transcriptional repression identifies novel targets and distinctions from E2F action. *Cancer Res* 62:6587-6597.

9. Markey, M.P., Bergseid, J., Bosco, E.E., Stengel, K., Xu, H., Mayhew, C.N., Schwemberger, S.J., Braden, W.A., Jiang, Y., Babcock, G.F., et al. 2007. Loss of the retinoblastoma tumor suppressor: differential action on transcriptional programs related to cell cycle control and immune function. *Oncogene* 26:6307-6318.

10. Barrett, T., Troup, D.B., Wilhite, S.E., Ledoux, P., Rudnev, D., Evangelista, C., Kim, I.F., Soboleva, A., Tomashevsky, M., and Edgar, R. 2007. NCBI GEO: mining tens of millions of expression profiles--database and tools update. *Nucleic Acids Res* 35:D760-765.

11. Shen, H., Powers, N., Saini, N., Comstock, C.E., Sharma, A., Weaver, K., Revelo, M.P., Gerald, W., Williams, E., Jessen, W.J., et al. 2008. The SWI/SNF ATPase Brm is a gatekeeper of proliferative control in prostate cancer. *Cancer Res* 68:10154-10162.

12. Irizarry, R.A., Bolstad, B.M., Collin, F., Cope, L.M., Hobbs, B., and Speed, T.P. 2003. Summaries of Affymetrix GeneChip probe level data. *Nucleic Acids Res* 31:e15.

13. Dai, M., Wang, P., Boyd, A.D., Kostov, G., Athey, B., Jones, E.G., Bunney, W.E., Myers, R.M., Speed, T.P., Akil, H., et al. 2005. Evolving gene/transcript definitions significantly alter the interpretation of GeneChip data. *Nucleic Acids Res* 33:e175.

14. Holcomb, I.N., Young, J.M., Coleman, I.M., Salari, K., Grove, D.I., Hsu, L., True, L.D., Roudier, M.P., Morrissey, C.M., Higano, C.S., et al. 2009. Comparative analyses of chromosome alterations in soft-tissue metastases within and across patients with castration-resistant prostate cancer. *Cancer Res* 69:7793-7802.

15. True, L., Coleman, I., Hawley, S., Huang, C.Y., Gifford, D., Coleman, R., Beer, T.M., Gelmann, E., Datta, M., Mostaghel, E., et al. 2006. A molecular correlate to the Gleason grading system for prostate adenocarcinoma. *Proc Natl Acad Sci U S A* 103:10991-10996.